XII International Conference on Computational Plasticity. Fundamentals and Applications
COMPLAS XII
E. Oñate, D.R.J. Owen, D. Peric and B. Suárez (Eds)

SIMULATION OF MATERIAL CONSEQUENCES INDUCED BY FSW FOR A TRIGONAL PIN

J.C. ROUX, E. FEULVARCH AND J.M. BERGHEAU

Université de Lyon, ENISE, LTDS, UMR 5513 CNRS
58 rue Jean Parot, 42023 Saint-Etienne cedex 2, France
e-mail: jean-christophe.roux@enise.fr, eric.feulvarch@enise.fr, jean-michel.bergheau@enise.fr

Key words: Friction Stir Welding, Finite Element, Meshing technique, Advection Equation

Abstract. The numerical simulation of Friction Stir Welding processes involves the coupling of a solid mechanics approach under large strains and large strain rates and heat transfer. The eulerian formalism leads to specially efficient finite element simulations of the matter flow under steady conditions. But with such a formulation, the calculation of the consequences induced by the stirring on the material (stirred state, microstructure, etc.) requires the coupling of advection equations for integrating the associated state variables. In this paper, a moving mesh strategy is proposed for the numerical simulation of Friction Stir Welding and material consequences, for complex pin's geometries. The numerical processing is detailed and the efficiency of the proposed method is discussed on a Friction Stir Welding simulation of 7075 series aluminum alloy.

1 Introduction

Numerical simulation of friction stir welding process is of growing interest in industry due to its ability to give an assembling solution in situations where all others conventional welding processes fail. This simulation needs to couple a solid mechanics approach under large strains and large strain rates with heat transfer so as to account for the temperature raise coming from the dissipated viscoplastic power and the friction between the pin and the matter. Several finite element formulations have been proposed to simulate the matter flow during the process. With a lagrangian formalism, an explicit step by step analysis is performed to follow the rotation of the pin. If such simulations give useful informations for the stage corresponding to the penetration of the pin into the material, it leads to very time consuming simulations to get the material flow under steady conditions. In addition, as the mesh follows the matter flow, the large distortions of the latter leads to unacceptable element distortions and the local modeling of thermal and mechanical effects requires very fine meshes in the vicinity of the stirring zone leading to significant size problems. This can

be avoided by means of a re-meshing procedure refining discretization only in the vicinity of the welding zone but this again increases the computing time. The Arbitrary Lagrangian Eulerian approach (ALE) can be used to obtain realistic computation times [1, 2, 3]. This consists in introducing a relative velocity between the mesh and the base material in order to decrease the distortions of the mesh. An alternative approach consists in using meshless techniques such as the Smoothed-Particle Hydrodynamics (SPH) [4, 5] or the Moving Particle Semi-implicit (MPS) method [6]. Anyway, as transient simulations must be performed, these approaches are complicated to implement and very time consuming [1, 7].

As most of welding processes, the Friction Stir Welding process involves a small size welding zone compared to that of the studied structure. It is very often assumed that a steady state is reached when the welded structure displays a translational geometry on a long distance. Therefore, the thermo-mechanical fields during the steady phase of the process can be calculated using a steady analysis with a reference frame linked to the welding velocity in an Eulerian formalism [8, 9, 10, 11], thus significantly reducing the computational efforts by avoiding the transient analysis. But it is obvious that such a steady state can only exist with axisymmetric tools.

For non-axisymmetric tools, a periodic state can be assumed, whose period depends on the tool's geometry. In this case, the finite element simulation of the periodic phase of the process can be achieved within an Eulerian formalism coupled with a simple moving mesh technique as suggested by Feulvarch *et al.* [12]. The mesh is composed of 2 parts : a first one which is fixed around the stirring zone and a second one which includes the base material near the tool and moves with a rotational solid motion corresponding to the tool's rotational velocity. Therefore, there are no mesh distortions. Moreover, the Eulerian formalism leads to satisfactory computing times which constitute a real numerical challenge [13].

The main difficulty induced by the Eulerian formalism is that the history of the material is not known a priori. Indeed, the mesh does not follow the material. Thus, the history of the material must be integrated for knowing the state of the base material at any point of the workpiece in terms of level of stirred state or other physical quantities such as those linked to the microstructure. These quantities are not just interesting in the post-processing of a thermomechanical computation but also during the thermomechanical simulation itself because the material behavior may depend on them. To overcome this difficulty, we propose in this paper, to couple the thermomechanical problem with an advection equation. Unfortunately, it will be shown that the moving mesh technique initially proposed by Feulvarch *et al.* does not properly handle the advection equation for numerical considerations. A variant of this approach is thus proposed so as to treat the advection problem. At last, the capacity of the method proposed is discussed in the case of the friction stir welding simulation of 7075 series aluminum alloy.

2 Physical model

2.1 Material flow

The material flow is governed by the momentum balance equation where inertial effects are neglected. For the momentum equation, it is possible to adopt Stokes assumption by considering that viscous stresses are predominant [14]. Within this framework, the momentum equation is given by :

$$\mathbf{div}(\sigma) = \mathbf{0} \tag{1}$$

where σ is the Cauchy stress tensor.

The mechanical behavior law must be able to represent both the pasty behavior in the vicinity of the tool and the plastic behavior with infinitesimal distortions on the edges of the iron sheets. Within the Eulerian formalism, the material is modeled as a temperature dependent non Newtonian fluid through the following relation :

$$\mathbf{S} = 2\,\mu\,\mathbf{D} \tag{2}$$

where $\mathbf{S}$ is the deviatoric stress tensor, μ is the dynamic viscosity and $\mathbf{D}$ is the strain rate tensor.

Viscosity can be defined in different ways. The simplest approach consists in assuming that stresses only depend on the strain rate, and not on the strain itself, through the Norton-Hoff law. It involves the consistency K of the base material as well as the sensitivity m to the strain rate, both parameters being temperature dependent :

$$\mu = K\,(\sqrt{3}\,D_{eq})^{m-1} \tag{3}$$

where $D_{eq} = \sqrt{2/3\,\mathbf{D} : \mathbf{D}}$ represents the equivalent strain rate.

Modeling the tool-material mechanical contact is certainly one of the most complex aspects. The thickness of the boundary layer is estimated to be 1mm maximum around the tool. Various models can be used to treat this boundary layer trough a friction coefficient, such as Norton's model, for instance, which is very similar to Norton-Hoff behavior law [1] :

$$\tau = \beta\,K\|\mathbf{v}_{tool} - \mathbf{v}\|^{q-1}\,(\mathbf{v}_{tool} - \mathbf{v}) \tag{4}$$

where β is a coefficient related to the nature of the interface and q is the sensitivity of the tangent stress τ at the sliding velocity $\mathbf{v}_{tool} - \mathbf{v}$. $\mathbf{v}_{tool}$ and $\mathbf{v}$ correspond respectively to the local velocity of the tool and the material outside the boundary layer.

2.2 Heat transfer

Friction Stir Welding involves no external heat source. Dissipation due to stirring of the material and its friction on the tool are sufficient to cause temperature rise in the macroscopic scaling thus allowing welding in the solid state. Heat transfer is governed by the heat equation :

$$Q + \mathrm{div}(\lambda\ \mathbf{grad}\,T) = \rho\,C\,\frac{\partial T}{\partial t} + \rho\,C\ \mathbf{v}_{cv}\ \mathbf{grad}\,T \tag{5}$$

where Q denotes the volumetric source term ; λ denotes the thermal conductivity ; ρ is the volumetric density ; C is the specific heat ; T is the temperature ; $\mathbf{v}_{cv}$ is the convective velocity corresponding to the Eulerian formalism.

The partial derivative problem governing thermomechanical coupling consists in juxtaposing the partial derivative problem related to heat diffusion with the problem related to mechanical phenomena. Both problems are coupled by :

- the mechanical power dissipated, involved as an internal source term in the heat equation,
- the influence of the material flow velocity on the thermal convection term,
- the temperature dependence of the mechanical behavior.

The volumetric source term Q involved in the heat equation corresponds to the mechanical power dissipated per unit volume. It can be expressed from the stress and the strain rate as follows :

$$Q = \alpha \, \mathbf{S} \, : \, \mathbf{D} \tag{6}$$

where α is the Taylor-Quinney coefficient ranging from 0.9 to 1 corresponding to the part of the mechanical power dissipated as heat.

With regard to heat transfer, the heat flux received by the welded sheets from the ambient air is modeled from a heat exchange coefficient H_{ext}. Likewise, modelling the thermal contact between the sheets and the welding support is performed by means of an exchange coefficient $H_{contact}$. With regard to the tool-material interface, the heat dissipated resulting from the friction of the matter on the tool is given by :

$$q_{interface} = \alpha \, \tau \, (\mathbf{v}_{tool} - \mathbf{v}) \tag{7}$$

α has been defined in (6) and is also taken into account in this expression as the mechanical power does not entirely dissipate as heat in the boundary layer. A part $\alpha_{material}$ of the heat dissipated is received by the base material and the other part is absorbed by the tool. As the thermo-mechanical coupling involved by Friction Stir Welding is very strong, the thermal and mechanical analyses must be performed simultaneously.

2.3 Integration of the material's history

The simulation of the mechanical properties after welding requires to know the history of the material. Different approaches can be used to integrate the history of the material in an Eulerian formalism. The first one consists in integrating the physical quantities along the trajectories corresponding to the stream lines in a stationnary configuration [10, 15]. This is not easy to do in 3D. An alternative approach consists in using an advection equation. This technique does not require any integration of the physical quantities along the trajectories passing through each integration point of the elements of the finite element mesh. Let's assume that the physical quantity observed is governed by a differential equation of the following type (phase proportions, fraction of hardened precipitates,

equivalent strain,...) :

$$\frac{du}{dt} = \mathcal{F}\left(u, T, \frac{dT}{dt}, \mathbf{D}, \dots\right) \tag{8}$$

In the context of the Eulerian formalism, this leads to

$$\frac{\partial u}{\partial t} + \mathbf{v}_{cv}\,\mathbf{grad}\; u = \mathcal{F}\left(u, T, \frac{dT}{dt}, \mathbf{D}, ...\right) \tag{9}$$

This expression constitutes the advection equation. The solution of this equation gives the distribution of u in space at each time step without needing to compute the trajectories of the material during the welding step and the rotation of the tool. In this paper, we propose to apply this formulation to compute the equivalent strain ε_{eq}. The interest of integrating the equivalent strain is that it can allow access to the stirred state of the material after welding and therefore the state of restoration for hardened alloys.

3 Finite element modeling

3.1 Discretization

To model the incompressible non Newtonian flow, finite element modeling faces a numerical difficulty. The discretization used must be chosen in a sensible way to avoid locking phenomena leading to an unrealistic solution. From a mathematical point of view, this can be explained by the fact that the velocity field must be sufficiently rich to satisfy both strain balance and incompressibility. In this work, the set of equations is solved using a tetrahedral element P1+/P1 detailed in [16], with which it is very easy to create a mesh for tools with complex geometries. This element is known to be very efficient in the context of large strain and strain rates. For this tetrahedral element, the discrete fields of pressure, temperature and equivalent strain are linear and continuous :

$$p^h(\mathbf{x}) = \sum_{i=1}^{N} p_i^h\, N_i(\mathbf{x}) \quad ; \quad T^h(\mathbf{x}) = \sum_{i=1}^{N} T_i^h\, N_i(\mathbf{x}) \quad ; \quad \varepsilon_{eq}^h(\mathbf{x}) = \sum_{i=1}^{N} \varepsilon_{eq_i}^h\, N_i(\mathbf{x}) \tag{10}$$

In these expressions, N denotes the number of nodes ; p_i^h, T_i^h and $\varepsilon_{eq_i}^h$ the values of the functions p^h, T^h and ε_{eq}^h at node i and $N_i(\mathbf{x})$ the shape function associated to this node. The approximation of the velocity is as follows :

$$\mathbf{v}^H(\mathbf{x}) = \sum_{i=1}^{N} \mathbf{v}_i^h\, N_i(\mathbf{x}) + \sum_{j=1}^{M} \mathbf{v}_j^b\, N_j^b(\mathbf{x}) \tag{11}$$

where M is the number of elements, $\mathbf{v}_i^h$ the value of the velocity at node i. $\mathbf{v}_j^b$ is the velocity value at each added internal node and $N_j^b(\mathbf{x})$ denotes the associated shape function which equal to zero on the element boundaries. An implicit (backward) Euler algorithm tolerating relatively large time steps is adopted for time integration of the temperature and the equivalent strain [17] : This discretization has the advantage of being unconditionally stable.

3.2 Weak formulation

To apply the finite element method, the weak integral formulation of the coupled problem is written in the discrete form as follows :

Find functions T^h, $\mathbf{v}^H$, p^h, ε_{eq}^h *such as for all functions* ϕ^h, $\mathbf{w}^H$, q^h, ψ^h

$$\left\{\begin{array}{ll}
\displaystyle\int_\Omega \rho\, C \frac{\partial T^h}{\partial t}\, \phi^h \,\mathrm{d}V + \int_\Omega \rho\, C\, \mathbf{v}_{cv} \,.\, \mathbf{grad}\, T^h \,(\phi^h + \eta^h)\,\mathrm{d}V & \\
\displaystyle + \int_\Omega \lambda\, \mathbf{grad}\, T^h \,.\, \mathbf{grad}\, \phi^h \,\mathrm{d}V - \int_\Omega Q \phi^h \,\mathrm{d}V - \int_{\partial\Omega_q} q\, \phi^h \,\mathrm{d}S & = 0 \\
\displaystyle\int_\Omega 2\,\mu\, \mathbf{D}(\mathbf{v}^H) : \mathbf{D}(\mathbf{w}^H)\,\mathrm{d}V - \int_\Omega p^h \,\mathrm{div}(\mathbf{w}^H)\,\mathrm{d}V - \int_{\partial\Omega_\tau} \mathbf{w}^H\, \tau \,\mathrm{d}S & = 0 \\
\displaystyle\int_\Omega q^h \,\mathrm{div}(\mathbf{v}^H)\,\mathrm{d}V & = 0 \\
\displaystyle\int_\Omega \frac{\partial \varepsilon_{eq}}{\partial t}^h \psi^h \,\mathrm{d}V + \int_\Omega \left(\mathbf{v}_{cv} \,.\, \mathbf{grad}\, \varepsilon_{eq}^h\right)\, (\psi^h + \xi^h)\,\mathrm{d}V - \int_\Omega D_{eq}\, \psi^h \,\mathrm{d}V & = 0
\end{array}\right. \tag{12}$$

where ϕ^h, $\mathbf{w}^H$, q^h and ψ^h are discrete test fields builded respectively in the same way as T^h, $\mathbf{v}^H$, p^h and ε_{eq}^h. To deal with the advection term, η^h and ξ^h are discrete test fields defined from the SU method (Streamline-Upwind).

3.3 Moving mesh strategy

As explained in the previous sections, the thermo-mechanical phenomena are strongly coupled. In order to solve this problem, a staggered approach could be used where the thermal problem and the mechanical problem are treated independently. But the importance of the couplings incites to prefer an approach where both problems are treated simultaneously to obtain the spatial distributions of temperature and velocity. Then, the equivalent strain can be computed using the advection equation. If the material behavior depends on the equivalent strain, a fully coupled approach could be used but this is not the case for the example proposed in the last part of this paper. Therefore, the thermomechanical problem does not depend on the results of the advection problem. So, the calculation of the equivalent strain is performed in a second step using the equivalent strain rate resulting from the thermomechanical computation.

For complex tool geometries, the computation can be carried out using the moving mesh strategy proposed by Feulvarch *et al.* [12]. This approach is based on a partition of the mesh in 2 parts as shown in figure 1 : a first one called Ω_1 which is fixed around the stirring zone and a second one called Ω_2 which includes the base material in contact with the tool. The second part Ω_2 is circular with a radius R_{Ω_2} and moves with a rotational solid motion at a rotational velocity equal to the one of the tool. Heat transfer is computed on

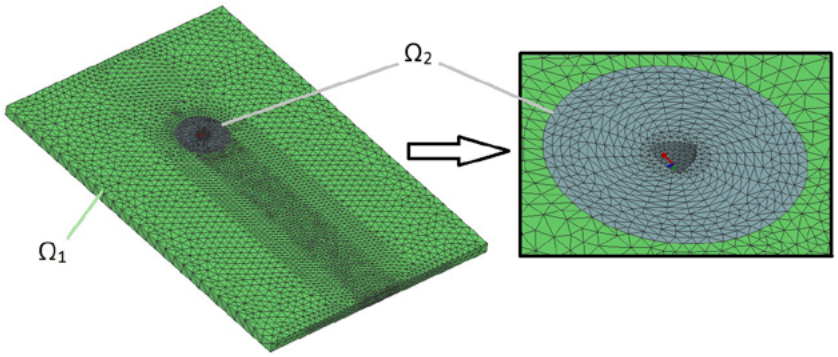

FIGURE 1: Partition of the mesh for the moving mesh technique of Feulvarch *et al.* [12].

the whole mesh, while the mechanical stirring is modeled only in the second moving part, to reduce the size of the numerical problem. The computations are assumed to converge on the periodic state without special consideration on the initial conditions. Considering the kinematics of the parts of the mesh, we get :

$$\begin{cases} \mathbf{v}_{cv} = -\mathbf{v}_{welding} & \text{in } \Omega_1 \\ \mathbf{v}_{cv} = \mathbf{v} - \omega \wedge \mathbf{r} & \text{in } \Omega_2 \end{cases}$$

where $\mathbf{v}_{welding}$ denotes the advance speed of the tool, ω the vector of rotation speed of the tool and $\mathbf{r}$ is the vector giving the position relative to the axis of rotation of the tool assumed perpendicular to the upper faces of sheets. Unfortunately, this approach can lead to velocities of mesh much bigger than the velocity of the material at the periphery of the movable part Ω_2 :

$$||\omega \wedge \mathbf{r}|| >> ||\mathbf{v}|| \quad \Rightarrow \quad \mathbf{v}_{cv} \approx -\omega \wedge \mathbf{r} \quad \text{in } \Omega_2$$

The material velocity then becomes negligible compared to that of the mesh. In this case, the convection associated to the material flow which plays a very important role in Eulerian formalism is not properly computed. This numerical phenomenon was not visible on the thermomechanical results shown in [12] because the convection term is not dominant compared to the diffusion term in heat transfer (low Peclet number). Moreover, the authors showed that two different radius of the domain Ω_2 ($R_{\Omega_2} = 12mm$ and $R_{\Omega_2} = 15mm$) lead to similar thermal results. To avoid this problem for the advection equation, we propose to reduce the radius of the moving part to decrease the maximum velocity of the mesh. This is achieved without reducing the size of the subdomain on which the mechanical stirring is modeled. So, a partition of the mesh in 3 parts as shown in figure 2 for a trigonal pin is now considered :

- a first one Ω_1 which is fixed around the stirring area ;
- a second one Ω_{2a} which is fixed and includes a part of the welding zone ;
- a third one Ω_{2b} which rotates and includes the rest of the welding zone very close to the pin.

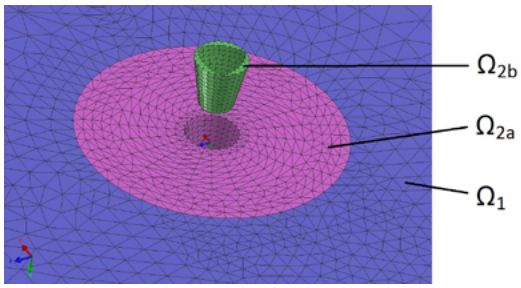

FIGURE 2: New partition of the mesh.

The part Ω_{2b} shown in figure 2 is circular with a radius as small as possible which corresponds to the envelop of the pin. With this new partition, we get :

$$\begin{cases} \mathbf{v}_{cv} = -\mathbf{v}_{welding} & \text{in } \Omega_1 \\ \mathbf{v}_{cv} = \mathbf{v} & \text{in } \Omega_{2a} \\ \mathbf{v}_{cv} = \mathbf{v} - \omega \wedge \mathbf{r} & \text{in } \Omega_{2b} \end{cases}$$

From the discretization point of view, the global mesh is built in such a way that it stays consistent at each angular position of Ω_{2b} during its rotation. Connections between parts in terms of temperature, velocity, pressure and equivalent strain are carried out with a penalty technique. With this approach, $||\omega \wedge \mathbf{r}||$ stays comparable to $||\mathbf{v}||$ everywhere in Ω_{2b}. Therefore, the convection due to material flow is correctly taken into account in the simulation compared to the convection due to the kinematic of the mesh.

4 Application to FSW of alloy 7075 with a trigonal pin

The new moving mesh technique is applied to the simulation of FSW of 7075 aluminum sheets. This application is similar to the one proposed in [12]. The tool has a trigonal pin and a flat shoulder with a radius equal to $10\,mm$. The tool axis is perpendicular to the upper faces of the sheets to be welded. In this example, the mesh is composed of 41 648 nodes and 231 206 elements, and it has been shown in [12] that an external radius of $12mm$ for Ω_{2a} is sufficient to accurately compute thermomechanical results. All physical data are given in appendix.

Figure 3 shows the temperature distribution on the welding plane with a welding velocity of 5 $mm.s^{-1}$ and a rotation speed equal to $500\,rpm$. All results are similar to the ones already obtained by Feulvarch *et al.* [12] and the periodic state is also reached after 10 rotations of the pin which corresponds to a computation time lower than 7 hours on a standard Intel(R) Core(TM)2 duo 2.53GHz PC with 4Go memory. For the proposed new approach, the maximum velocity of the mesh is located at the maximum radius of Ω_{2b} which is equal to $3mm$. This leads to a maximum value of about $||\omega \wedge \mathbf{r}|| \approx 157mm.s^{-1}$ comparable to the maximum computed material velocity of about $||\mathbf{v}|| \approx 50mm.s^{-1}$. For the moving mesh technique firstly proposed in [12], the maximum velocity of the mesh for $R_{\Omega_2} = 12mm$ was about $||\omega \wedge \mathbf{r}|| \approx 628mm.s^{-1}$. This value is bigger by several orders of

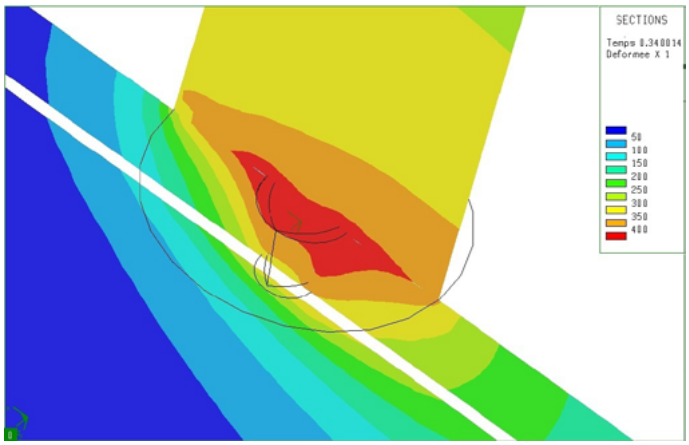

FIGURE 3: Temperature distributions (°C) in the welding plane in the tool, the aluminum sheets and the backing plate.

magnitude than the material velocity equal to $5mm.s^{-1}$. The convection in the orthoradial direction linked to the motion of the mesh is then predominant compared to convection due to the material flow. This leads to an unrealistic and oscillating distribution of equivalent strains as shown in figure 4*(a)* obtained by solving the advection problem. Indeed, for this result obtained at time $0.23s$, the equivalent strain varies between -8000% and 15000% while the equivalent strain must be positive. Whatever the simulation time, the equivalent strain is concentrated around the pin while the material convection is supposed to lead to a comet-shaped distribution. It is obvious that the distribution plotted in figure 4*(a)* does not correspond to physical reality. With the method developped, the comet-shaped distribution of the equivalent strain clearly appears in figure 4*(b)*. One can note that the equivalent strain is of the same order than the one obtained by Assidi *et al.* [1].

5 Conclusion

In this article, a coupling between thermomechanical calculation and an advection equation has been proposed, for integrating the material history in an Eulerian formalism. It is shown that the moving mesh strategy initially proposed by Feulvarch *et al.* [12] must be adapted so as to accurately integrate the advection equation associated to the physical quantities of interest. It is suggested to decompose now the mesh in 3 parts : a part very near to the pin which rotates with the pin, a second part around the first one needed for the mechanical computation and a third part including the rest of the aluminum sheets needed to model heat transfer. The efficiency of the proposed approach is shown in an application of Friction Stir Welding of 7075 aluminum sheets with a trigonal pin, for calculating the equivalent strain in the whole structure giving useful information on the stirred state of the material. The same approach can now be used to calculate other useful physical quantities such as those associated with microstructure through adequate kinetics equations.

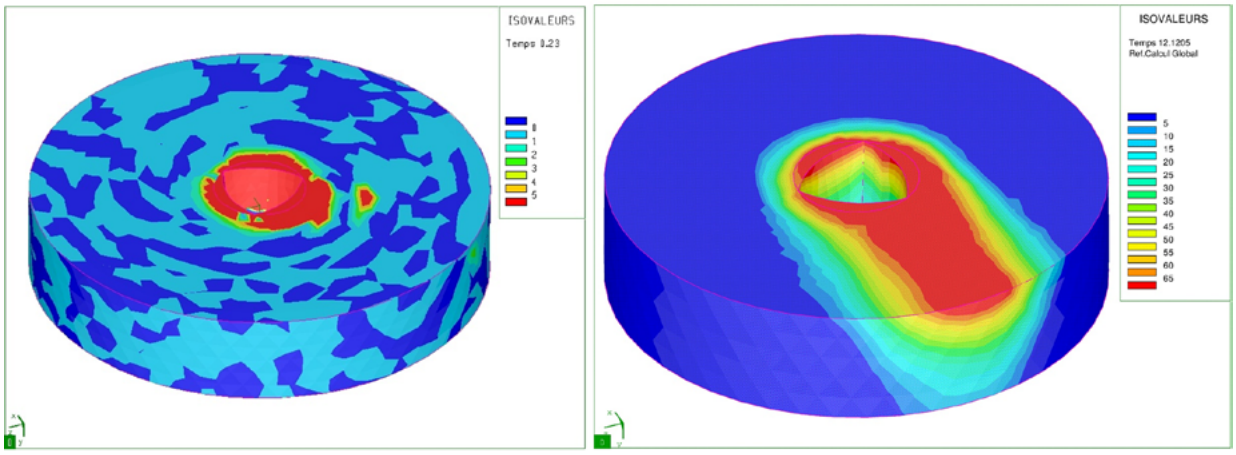

FIGURE 4: *(a)* Equivalent strain distribution in Ω_2 obtained with the moving mesh technique proposed in [12] - *(b)* Equivalent strain distribution in Ω_{2a} and Ω_{2b} obtained with the new technique.

RÉFÉRENCES

[1] M. Assidi, L. Fourment, S. Guerdoux, T. Nelson, *Friction model for friction stir welding process simulation : Calibrations from welding experiments*, International Journal of Machine Tools & Manufacture, vol. 50, 143-155, 2010.

[2] A. Timesli, B. Braikat, H. Zahrouni, A. Moufki, H. Lahmam, *Toward friction stir welding simulation using moving least square technique*, Proc of the 2nd International Conference on Friction Stir Welding and Processing FSWP'2012, ISBN 978-2911256-72-1, 119-121, 2012.

[3] T. Heuzé, J.B. Leblond, J.M. Bergheau, E. Feulvarch, *A finite element for laminar flow of incompressible fluids with inertia effects and thermomechanical coupling*, European Journal of Computational Mechanics, vol. 19, 293-304, 2010.

[4] A. M Tartakovsky, G. Grant, X. Sun and M. Khaleel, *Modeling of Friction Stir Welding (FSW) Process with Smooth Particle Hydrodynamics (SPH)*, SAE 2006 World Congress, Detroit, USA, 2006.

[5] O. Lorrain, J. Serri, V. Favier, H. Zahrouni, M. El Hadrouz, *A contribution to a critical review of FSW numerical simulation*, Journal of Mechanics of Materials and Structures, vol. 4, 351-369, 2009.

[6] G. Yoshikawa, F. Miyasaka, Y. Hirata, Y. Katayama, T. Fuse, *Development of numerical simulation model for FSW employing particle method*, Science and Technology of Welding and Joining, 17(4), 255-263, 2012.

[7] H. Schmidt, J. Hattel., *A local model for the thermomechanical conditions in friction stir welding*, Modell. Simul. Mater. Sci. Eng., vol. 13, 77-93, 2005.

[8] P. A. Colegrove, H. R. Shercliff, *Development of Trivex friction stir welding tool - Part 1 and 2*, Science and Technology of Welding and Joining, 9(4), 345-361, 2004.

[9] D. Jacquin, B. de Meester, A. Simar, D. Deloison, F. Montheillet, C. Desrayaud, *A simple Eulerian thermomechanical modeling of friction stir welding*, Journal of Materials Processing Technology, vol. 211, 57-65, 2011.

[10] A. Bastier, M.H. Maitournam, F. Roger, K. Dang Van, *Modelling of the residual state of friction stir welded plates*, Journal Material Processing Technology, vol. 200, 25-37, 2008.

[11] E. Feulvarch, V. Robin, F. Boitout, J.M. Bergheau, *A 3D finite element modelling for thermofluid flow in friction stir welding*, Mathematical modelling of weld phenomena 8, edited by H. Cerjack, H.K.D.H. Bhadeshia, E. Kozeshnik, ISBN 978-3-902465-69-6, 711-724, 2007.

[12] E. Feulvarch, J.-C. Roux, J.-M. Bergheau, *A simple and robust moving mesh technique for the finite element simulation of Friction Stir Welding*, Journal of Computational and Applied Mathematics, vol. 246, 269-277, 2013.

[13] C. Tutum, J. H. Hattel, *Numerical optimisation of friction stir welding : review of future challenges*, Science and Technology of Welding and Joining, 16(4), 318-324, 2011.

[14] H. R. Shercliff, P. A. Colegrove, *Modelling of Friction Stir Welding*, Mathematical modelling of weld phenomena, vol. 6, 927-974, 2002.

[15] J.-M. Bergheau, G. Mangialenti, F. Boitout, *Contribution of numerical simulation to the analysis of heat treatment and surface hardening processes*, Proc. of Heat Treat'98, 18th ASM Heat Treating Society Conference and Exposition, ASM International, 681-690, 1998.

[16] E. Feulvarch, N. Moulin, P. Saillard, T. Lornage, J.-M. Bergheau, 3D simulation of glass forming process, Journal of Materials Processing Technology, vol. 164165, 1197-1203, 2005.

[17] E. Feulvarch, J.M. Bergheau, *An implicit-fixed grid method for the finite element analysis of heat transfer involving phase changes*, Numerical Heat Transfer - Part B : Fundamentals, 51(6), 585-610, 2007.

[18] Jin Z., Cassada W. A., Cady C. M., Gray G. T., *Mechanical Response of AA7075 Aluminium Alloy over aWide Range of Temperatures and Strain Rates*, Material Science Forum, vol. 331-337, 527-532, 2000.

Appendix – Material data

In the literature, it is difficult to find data related to consistency K and sensitivity m (see section 2.1) to the strain rate occurring in Norton-Hoff law expression on the temperature range of FSW. For alloy 7075, Jin *et al.* measure the flow stress variation

by means of compression tests at strain rates ranging from $0.001\,\mathrm{s}^{-1}$ to $2100\,\mathrm{s}^{-1}$ and temperatures ranging from 23° C to 470° C [18]. In the example of section 4, consistency and sensitivity have been determined from these evolutions and are given in table 1. The

$T\ (°C)$	20	200	300	400	470
$K\ (MPa^m)$	630	440	145	83	30
m	0	225.10^{-4}	708.10^{-4}	127.10^{-3}	146.10^{-3}

TABLE 1: Values of the material consistency K and its strain rate sensitivity m as functions of temperature for the Norton-Hoff model.

thermal characteristics are given in tables 2 and 3. The emissivity of the tool and backing plate is equal to 0.05 and the one of the aluminum alloy is 0.88. In equation (4), $\beta\,K$ and q are taken equal respectively to 5 $\mathrm{MPa}^{\mathrm{q}}$ and 0.25 for the modeling of the mechanical contact between the tool and the sheets. Considering the effusivity of the materials in contact, the sheets are assumed to receive about 60% of the power dissipated by friction at the interface. For heat exchanges with the welding support, the value of $H_{contact}$ depends on temperature, contact pressure, and on the nature of the materials in contact and many other parameters such as surface states. That is why literature reveals a very wide range of values. In this application, $H_{contact}$ is considered equal to $1000\ \mathrm{W\,m^{-2}\,K^{-1}}$.

$T\ (°C)$	20	120	220	320	420	470
$\rho\ (kg/m^3)$	2750	2730	2710	2690	2660	2650
$C\ (J/kg/K)$	850	910	960	980	1040	1100
$\lambda\ (W/m/K)$	130	139	146	155	163	170

TABLE 2: Thermal properties of 7075 aluminum alloy.

$T\ (°C)$	20	200	400	500
$\rho\ (kg/m^3)$	7850	7800	7730	7690
$C\ (J/kg/K)$	450	550	610	650
$\lambda\ (W/m/K)$	68	59	47	41.5

TABLE 3: Thermal properties of tool and backing plate.